Algorithms for the calculation of psychrometric properties from multi-fluid Helmholtz-energy-explicit models[☆]

Ian H. Bell[a,*], Eric W. Lemmon[a], Allan H. Harvey[a]

[a] *Applied Chemicals and Materials Division, National Institute of Standards and Technology, Boulder, CO, 80305, USA*

Abstract

Psychrometric properties of humid air are widely used in the analysis and modeling of thermal systems. In this work, we present a method for obtaining these properties from the multi-fluid mixture formulation of the GERG mixture model. This mixture model was originally developed to model the thermodynamics of natural gas mixtures, and more recently has been extended to model thermodynamic properties relevant for carbon capture and storage. The primary advantage of this formulation is that the dry air composition is not fixed, and can be adjusted to suit the application, for instance for combustion flue gases, for air in submarines, for Martian atmospheres, etc. Furthermore, this multi-fluid framework employs the highest accuracy pure-fluid equations of state in the literature.

We present algorithms that can be used to calculate the quantity of water in the saturated vapor in vapor-liquid and solid-vapor equilibria, and other properties that arise out of these equilibria calculations, such as relative humidity and humidity ratio. We also present algorithms for converting other common sets of independent variables (e.g., wet-bulb temperatures), to the natural variables of the mixture model.

Comprehensive discussion of the developed algorithms is provided, as well as sample code in the C++ language.

---

1. Introduction

Psychrometry is the study of the thermodynamic properties of mixtures of water and air. There have been a number of formulations of the psychrometric properties of humid air proposed over the years, with varying levels of complexity and accuracy (Wexler et al., 1983; ASHRAE, 2001; Nelson and Sauer, 2002; Herrmann et al., 2009a). The work of Herrmann *et al.* (2009b) (page 53) provides an overview of the models that had been developed as of 2009. In the past, models have primarily used a simple virial expansion for the vapor-phase thermodynamics, and considered vapor-liquid and solid-vapor equilibria.

One of the nomenclature-related issues that constantly bedevils the discussion of psychrometric property evaluation is the fact that in most psychrometric evaluations, the thermodynamic properties are used on a per-unit-dry-air basis. Not all works are consistent or clear about their choice of nomenclature, and the distinction between properties defined on a per-unit-dry-air or per-unit-humid-air basis is one of the most frequent sources of confusion. In this work, the mixture model always considers the entire humid air mixture, and never the dry air by itself. Therefore, all properties derived from the mixture model are on a per-unit-humid-air basis.

For the subset of thermodynamic properties considered here, the distinction between per-unit-dry-air or per-unit-humid-air properties does not generally arise. In contrast, in many applications (e.g., the evaluation of cycle efficiency in a Brayton cycle), enthalpies and entropies are required. In that case, it is important to be explicit about whether properties are on a per-unit-dry-air or per-unit-humid-air basis.

This manuscript is laid out as follows: first we describe the dry air mixture composition and then the humid air mixture composition. Then we describe the thermodynamic models used for the pure components, and how these pure components are combined into a thermodynamic mixture model. Finally, we close with a description of the required phase equilibrium calculations and the determination of phase equilibria related properties. The conclusion of this work is the construction of a psychrometric chart for humid air at one atmosphere.

2. Air

2.1. Dry air composition

The composition of dry air is given on a mole fraction basis. Humid air can be modeled as a pseudo-binary mixture formed of water vapor and a fixed-composition dry

---

[☆] Contribution of the National Institute of Standards and Technology, not subject to copyright in the U.S. Commercial equipment, instruments, or materials are identified only in order to adequately specify certain procedures. In no case does such identification imply recommendation or endorsement by the National Institute of Standards and Technology, nor does it imply that the products identified are necessarily the best available for the purpose.

[*] Corresponding Author

Email addresses: `ian.bell@nist.gov` (Ian H. Bell), `eric.lemmon@nist.gov` (Eric W. Lemmon), `allan.harvey@nist.gov` (Allan H. Harvey)

NOMENCLATURE

Variables

A, B, C	Coefficient for Henry's law
a	Helmholtz energy ($\mathrm{J{\cdot}mol^{-1}}$)
f_e	Enhancement factor
f_i	Fugacity of component i (Pa)
f_i'	Liquid fugacity of component i (Pa)
f_i''	Vapor fugacity of component i (Pa)
F	Residual function
F_{ij}	Binary scaling factor
g	Molar Gibbs energy in joules per mole of humid air ($\mathrm{J{\cdot}mol^{-1}}$)
h	Molar enthalpy of humid air in joules per mole of humid air ($\mathrm{J{\cdot}mol^{-1}}$)
h''	Molar enthalpy of saturated vapor in joules per mole of humid air ($\mathrm{J{\cdot}mol^{-1}}$)
$h_{\mathrm{H_2O},0}$	Molar enthalpy of pure water or ice in joules per mole of water ($\mathrm{J{\cdot}mol^{-1}}$)
J	Massieu potential ($\mathrm{J{\cdot}K^{-1}}$)
$\mathbf{J}$	Jacobian matrix
k_H	Henry's law constant (Pa)
$m_{\mathrm{H_2O}}$	Mass of water (kg)
m_da	Mass of dry air (kg)
M_da	Molar mass of dry air in kg of dry air per mole dry air ($\mathrm{kg{\cdot}mol^{-1}}$)
M_ha	Molar mass of humid air in kg of humid air per mole humid air ($\mathrm{kg{\cdot}mol^{-1}}$)
n	Number of moles
N	Number of components in the mixture
p	Pressure (Pa)
$p_{\mathrm{sat,H_2O},0}$	Saturation pressure of pure water (Pa)
$p_{\mathrm{c},i}$	Critical pressure of the i-th fluid (Pa)
$\boldsymbol{r}$	Vector of residuals (-)
R	Universal gas constant ($\mathrm{J{\cdot}mol^{-1}{\cdot}K^{-1}}$)
T	Temperature (K)
T_db	Dry-bulb temperature (K)
T_dp	Dew-point temperature (K)
$T_{\mathrm{c},i}$	Critical temperature of the i-th fluid (K)
T_r	Reducing temperature (K)
T_R	Reduced temperature (-)
$T_{\mathrm{sat,H_2O},0}$	Saturation temperature of pure water (K)
T_wb	Thermodynamic wet-bulb temperature (K)
v_da	Volume per kg dry air ($\mathrm{m^3{\cdot}kg^{-1}}$)
$v_{\mathrm{c},i}$	Critical volume of the i-th fluid ($\mathrm{m^3{\cdot}mol^{-1}}$)
W	Humidity ratio in kg H_2O per kg dry air ($\mathrm{kg{\cdot}kg^{-1}}$)
$\boldsymbol{x}$	Array of mole fraction (-)
$\boldsymbol{X}$	Vector of independent variables (-)
x	Mole fraction (-)
x'	Mole fraction of liquid (-)
x''	Mole fraction of vapor (-)

Greek variables

α	Non-dimensionalized Helmholtz energy (-)
α^r	Non-dimensionalized residual Helmholtz energy (-)
$\alpha^\mathrm{r}_{\mathrm{o}i}$	Pure fluid Helmholtz energy (-)
α^r_{ij}	Binary departure function (-)
α^0	Non-dimensionalized ideal-gas Helmholtz energy (-)
β	Mixture interaction parameter (-)
δ	Reduced density (-)
γ	Mixture interaction parameter (-)
μ	Chemical potential ($\mathrm{J{\cdot}mol^{-1}}$)
ϕ	Relative humidity (-)
ω	Acentric factor (-)
ρ	Molar density of humid air in moles humid air per cubic meter ($\mathrm{mol{\cdot}m^{-3}}$)
ρ_r	Reducing density in moles humid air per cubic meter ($\mathrm{mol{\cdot}m^{-3}}$)
ρ_c	Critical density ($\mathrm{mol{\cdot}m^{-3}}$)
τ	Reciprocal reduced temperature (-)
τ^*	Critically reduced temperature $\tau^* = 1 - T_\mathrm{R}$ (-)

Subscripts

da	Dry air
ha	Humid air
i	Index
ice	Ice
j	Index
H_2O	Water
Ar	Argon
N_2	Nitrogen
O_2	Oxygen
CO_2	Carbon dioxide

Superscripts

r	Residual
0	Ideal-gas
$''$	Vapor phase
$'$	Liquid phase

air. While the exact composition of dry air varies slightly with time and location, the composition is dominated by the contributions from nitrogen, oxygen, and argon, which form more than 99.95% of the molar composition. The current international standard for the composition of dry air is that of Picard *et al.* (2008), which gives the composition presented in Table 1, yielding a molar mass of 0.02896546 kg·mol^{-1}. The molar masses of the minor constituents have been rounded as in Picard *et al.* (2008).

Table 1: Composition of dry air according to Picard *et al.* (2008)

Component	Mole fraction
N_2	0.780848
O_2	0.209390
Ar	0.009332
CO_2	0.00040
Ne	18.2×10^{-6}
He	5.2×10^{-6}
CH_4	1.5×10^{-6}
Kr	1.1×10^{-6}
H_2	0.5×10^{-6}
N_2O	0.3×10^{-6}
CO	0.2×10^{-6}
Xe	0.1×10^{-6}

In practice, the minor constituents of air can be neglected as they do not contribute significantly to the thermodynamics of the dry air mixture. It is common to keep only the top three or four constituents. In this work, we use a four-component dry air mixture with the composition as given in Table 2. This composition is obtained by fixing the composition of carbon dioxide at 400 ppm, and adding the 30 ppm from the eight minor constituents to the top three components[1], weighted by the product of the molar mass and mole fraction for the three primary constituents.

Table 2: Composition of dry air from its four major components

Component	Variable	M (kg·mol^{-1})	Mole fraction
N_2	$x_{\mathrm{da,N_2}}$	0.0280134	0.780871
O_2	$x_{\mathrm{da,O_2}}$	0.0319988	0.209397
Ar	$x_{\mathrm{da,Ar}}$	0.039948	0.009332
CO_2	$x_{\mathrm{da,CO_2}}$	0.04401	0.000400

The molar mass of dry air is obtained as a mole-fraction-weighted average of the molar masses of the constituents of dry air obtained from the fixed composition of dry air:

$$M_{\mathrm{da}} = x_{\mathrm{da,N_2}}M_{\mathrm{N_2}}+x_{\mathrm{da,O_2}}M_{\mathrm{O_2}}+x_{\mathrm{da,Ar}}M_{\mathrm{Ar}}+x_{\mathrm{da,CO_2}}M_{\mathrm{CO_2}}, \tag{1}$$

yielding a dry air molar mass of 0.02896570 kg·mol^{-1}, or a difference of 8.5 ppm from the value of 0.02896546 kg·mol^{-1} from Picard *et al.* (2008).

2.2. Humid air composition

The humid air mixture can then be treated as a binary mixture of water and dry air. For a given water mole fraction $x_{\mathrm{H_2O}}$, the dry air mole fraction is $x_{\mathrm{da}} = 1 - x_{\mathrm{H_2O}}$, and therefore the mixture mole fractions of the dry air components (in moles of the component per mole of humid air) are given by

$$x_{\mathrm{N_2}} = (1 - x_{\mathrm{H_2O}})x_{\mathrm{da,N_2}} \tag{2}$$

$$x_{\mathrm{O_2}} = (1 - x_{\mathrm{H_2O}})x_{\mathrm{da,O_2}} \tag{3}$$

$$x_{\mathrm{Ar}} = (1 - x_{\mathrm{H_2O}})x_{\mathrm{da,Ar}} \tag{4}$$

$$x_{\mathrm{CO_2}} = (1 - x_{\mathrm{H_2O}})x_{\mathrm{da,CO_2}}, \tag{5}$$

where the values of the mole fractions of the dry air constituents can be found in Table 2. The mole fractions of all the constituents of the mixture (water and the components of dry air) must therefore sum to unity:

$$x_{\mathrm{H_2O}} + x_{\mathrm{N_2}} + x_{\mathrm{O_2}} + x_{\mathrm{Ar}} + x_{\mathrm{CO_2}} = 1. \tag{6}$$

The molar mass of the humid air is then obtained as a mole-fraction-weighted average of the dry air and water molar masses

$$M_{\mathrm{ha}} = x_{\mathrm{H_2O}}M_{\mathrm{H_2O}} + (1 - x_{\mathrm{H_2O}})M_{\mathrm{da}}, \tag{7}$$

where the water molar mass $M_{\mathrm{H_2O}}$ is 0.018015268 kg·mol^{-1}(Wagner and Pruß, 2002). Unless otherwise specified, the composition of dry air is assumed to be fixed with the composition in Table 2.

In the C++ code presented in the supplemental material, the composition of the humid air can be altered, for instance, to be able to model the psychrometric properties of the Martian atmosphere as in Shallcross (2005).

3. Pure fluid thermodynamic properties

3.1. Pure fluid equations of state

The state-of-the-art equations of state (EOS) for pure substances are all of the Helmholtz-energy-explicit formulation[2]. This model is formulated in terms of the fundamental thermodynamic potential of Helmholtz energy; from this potential all other properties can be obtained as derivatives with respect to the independent variables.

The non-dimensionalized Helmholtz energy can be expressed as

$$\alpha(\tau, \delta) = \frac{a}{RT} = \alpha^0(\tau, \delta) + \alpha^{\mathrm{r}}(\tau, \delta), \tag{8}$$

---

[1] The molar composition in Table 1 does not sum to 1.0. The missing 2.9×10^{-6} is also included such that the composition of air used here will sum to unity.

[2] Rigorously, they are expressed in a Massieu-potential-explicit form, where the Massieu potential J is given as $J = -a/T$, but the literature currently describes this model as being of the Helmholtz-energy-explicit formulation, a convention that we follow.

where the independent variables in the Helmholtz energy potential (T and ρ) are transformed into reduced variables $\tau = T_c/T$ and $\delta = \rho/\rho_c$, α^0 is the ideal-gas contribution to the Helmholtz energy, and α^r is the residual contribution to the non-dimensionalized Helmholtz energy. From this potential, it is possible to evaluate all other thermodynamic properties; for instance the pressure can be evaluated from

$$p = \rho RT\left(1 + \delta\left(\frac{\partial\alpha^r}{\partial\delta}\right)_\tau\right), \tag{9}$$

the molar enthalpy from

$$\frac{h}{RT} = \tau\left[\left(\frac{\partial\alpha^0}{\partial\tau}\right)_\delta + \left(\frac{\partial\alpha^r}{\partial\tau}\right)_\delta\right] + \delta\left(\frac{\partial\alpha^r}{\partial\delta}\right)_\tau + 1, \tag{10}$$

and so on. More information on pure fluid equations of state can be found in the literature (Span, 2000).

The following substances are considered here, with the reference to their corresponding equation of state :

- water (H_2O) (Wagner and Pruß, 2002)
- nitrogen (N_2) (Span et al., 2000)
- oxygen (O_2) (Schmidt and Wagner, 1985)
- argon (Ar) (Tegeler et al., 1999)
- carbon dioxide (CO_2) (Span and Wagner, 1996)

The properties of each of these fluids are represented by a reference-grade equation of state (meaning the equation of state can generally replicate the highest accuracy experimental data to within their experimental uncertainty). These equations of state are in general valid from the zero-density limit to the melting and sublimation lines of the fluid; the range of available data constrains the maximum temperature or pressure of the EOS.

3.2. Water properties

The potential for equilibria between gaseous and solid phases must be taken into account for temperatures less than the triple point temperature of pure water. As a result, it is necessary to consider the phase of the water in equilibrium with the gaseous phase. Figure 1 shows a schematic of the phase boundary for the equilibrium between water's phases. For pressures below a few hundred MPa, the highest temperature at which ice can exist is the triple-point temperature of pure water, defined to be exactly 273.16 K. Above 208.6 MPa, other forms of ice can be found. Determination of whether the vapor phase is in equilibrium with a solid or liquid phase of water is rather complex, and described in greater detail below.

Feistel and Wagner (2006) give a fundamental reference-grade equation of state for the ice Ih phase of H_2O explicit in Gibbs energy, with temperature and pressure as independent variables. Wagner *et al.* (2011) give an equation for the melting line of ice Ih, defining the boundary between liquid and ice (though rigorously, one should find the melting line as the line satisfying equality of Gibbs energy between the equations of state of ice Ih and liquid water; the melting line of Wagner *et al.* (2011) gives only an approximation to this equilibrium condition). Wagner *et al.* (2011) also gives an equation for the sublimation curve for pure water.

One of the challenges when combining different thermodynamic models together, here further complicated by the application of a mixture model, is that the reference states for enthalpy (or internal energy) and entropy must agree for each equation of state. In this case, the three models (solid, fluid, mixture) all use the IAPWS-95 reference state, which is that liquid water at the solid(Ice Ih)/liquid/vapor triple point has entropy and internal energy equal to zero. As a result, the enthalpy equals 0.611872 kJ·kg^{-1} at this state point.

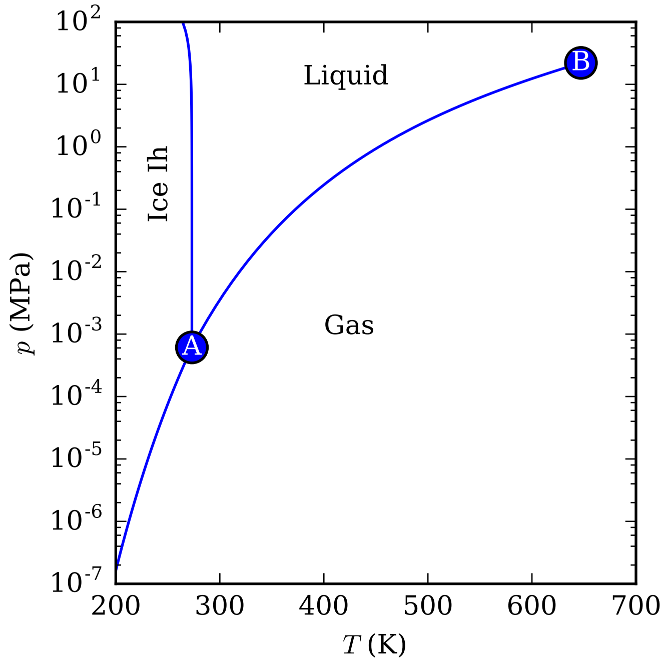

Figure 1: Phase equilibria diagram for pure H_2O [A: solid-liquid-vapor triple point (273.16 K, 611.657 Pa), B: Critical point (647.096 K, 22.064 MPa)]

Table 3: Binary interaction parameters employed in the EOS-CG model

Name$_1$	Name$_2$	$\beta_{T,ij}$	$\gamma_{T,ij}$	$\beta_{v,ij}$	$\gamma_{v,ij}$	F_{ij}	α^{r}_{ij}
N_2	CO_2	1.005895	1.107654	0.977795	1.047578	1.000000	Gernert and Span (2016)
N_2	H_2O	1.048054	0.805147	0.926245	0.733443	1.000000	Gernert and Span (2016)
N_2	Ar	0.999442	0.989311	1.006697	1.001549	0.000000	Gernert and Span (2016)
N_2	O_2	0.997191	0.995157	0.999522	0.997082	0.000000	Gernert and Span (2016)
CO_2	H_2O	1.030538	0.828472	1.021392	0.895156	1.000000	Gernert and Span (2016)
CO_2	Ar	1.027147	0.968781	1.001378	1.029710	1.000000	Gernert and Span (2016)
CO_2	O_2	1.000000	1.031986	1.000000	1.084460	0.000000	Gernert and Span (2016)
H_2O	Ar	0.679104	0.921000	0.940398	1.050952	0.000000	Gernert and Span (2016)
H_2O	O_2	0.798046	0.807842	0.972576	0.873460	0.601700	Gernert and Span (2016)
Ar	O_2	1.000962	0.988822	0.993540	1.001341	0.000000	Gernert and Span (2016)

Note: $\beta_{T,ij} = 1/\beta_{T,ji}$ and $\beta_{v,ij} = 1/\beta_{v,ji}$

4. Mixture thermodynamic properties

The mixture model is used to characterize the thermodynamic properties of the liquid and gaseous phases. In the case of vapor-liquid equilibrium, the mixture model is used to model both phases. In the case of solid-vapor equilibrium, the equation of state for pure ice is used to model the properties of the ice in equilibrium with the vapor phase.

4.1. Model formulation

The GERG (*Groupe Européen de Recherches Gazières*) mixture model is formulated based on mixing rules combining highly-accurate equations of state for the pure components forming the mixture as described above. This mixture model has been extensively described in the literature (Kunz et al., 2007; Kunz and Wagner, 2012). In recent years, Gernert and co-workers developed the EOS-CG model, extending the high-accuracy mixture formulations developed in the GERG model to binary pairs needed to model carbon capture and sequestration applications (Gernert et al., 2014; Gernert and Span, 2016).

The mixture model is also formulated in terms of the Helmholtz energy - as a sum of ideal-gas and residual contributions

$$\alpha(\tau,\delta,\boldsymbol{x}) = \frac{a}{RT} = \alpha^0(\tau,\delta,\boldsymbol{x}) + \alpha^{\rm r}(\tau,\delta,\boldsymbol{x}). \tag{11}$$

Unlike the pure fluids, the mixture model employs reduced temperatures $\tau = T_{\rm r}(\boldsymbol{x})/T$ and densities $\delta = \rho/\rho_{\rm r}(\boldsymbol{x})$ that are functions of the mixture composition. The empirical reducing functions can be given by

$$T_{\rm r}(\boldsymbol{x}) = \sum_{i=1}^{N} x_i^2 T_{{\rm c},i} + \sum_{i=1}^{N-1}\sum_{j=i+1}^{N} 2x_i x_j \frac{x_i + x_j}{\beta_{T,ij}^2 x_i + x_j} T_{ij} \tag{12}$$

$$v_{\rm r}(\boldsymbol{x}) = \sum_{i=1}^{N} x_i^2 v_{{\rm c},i} + \sum_{i=1}^{N-1}\sum_{j=i+1}^{N} 2x_i x_j \frac{x_i + x_j}{\beta_{v,ij}^2 x_i + x_j} v_{ij} \tag{13}$$

where

$$T_{ij} = \beta_{T,ij}\gamma_{T,ij}(T_{{\rm c},i}T_{{\rm c},j})^{0.5} \tag{14}$$

and

$$v_{ij} = \frac{1}{8}\beta_{v,ij}\gamma_{v,ij}\left(v_{{\rm c},i}^{1/3} + v_{{\rm c},j}^{1/3}\right)^3, \tag{15}$$

and where the adjustable interaction parameters $\beta_{T,ij}$, $\gamma_{T,ij}$, $\beta_{v,ij}$, and $\gamma_{v,ij}$ weight the critical properties of the pure fluids ($T_{{\rm c},i}$ and $v_{{\rm c},i}$) that form the ij binary pair.

The residual non-dimensionalized Helmholtz energy $\alpha^{\rm r}$ is given by the form

$$\alpha^{\rm r} = \sum_{i=1}^{N} x_i \alpha_{{\rm o}i}^{\rm r}(\tau,\delta) + \sum_{i=1}^{N-1}\sum_{j=i+1}^{N} x_i x_j F_{ij}\alpha_{ij}^{\rm r}(\tau,\delta), \tag{16}$$

where $\alpha_{{\rm o}i}^{\rm r}$ is the residual non-dimensionalized Helmholtz energy contribution from the i-th pure component evaluated at the mixture τ and δ, $\alpha_{ij}^{\rm r}$ is a mixture departure function for the ij binary pair, and F_{ij} is a constant weighting factor for the ij binary pair.

The interaction parameters and departure functions used in this work are summarized in Table 3. The interaction parameters and departure functions are taken from the EOS-CG model (Gernert and Span, 2016), which was developed to yield a comprehensive coverage of all thermodynamic properties relevant to these systems. The work of Gernert *et al.* gives a comprehensive listing of the experimental datasets that were considered in the development of EOS-CG, and the accuracy of reproduction of the experimental measurements.

It is known that the thermodynamic properties obtained from the EOS-CG model (e.g., enhancement factors) are not as accurate as some humid air property formulations that focus on humid air alone. In order to bring the accuracy of this model in line with other libraries, a fitting exercise is required that focuses exclusively on the vapor phase and does not attempt to also fit the other more complex phase equilibria behaviors that are possible (e.g., liquid-liquid equilibria, vapor-liquid-liquid equilibria, etc.). Fitting psychrometric-focused interaction parameters and departure functions remains the topic of future work. The topic of this paper is solely the *algorithms* that are required to *use* this sort of a model.

The range of validity of the proposed model is somewhat difficult to quantify, being a function of composition of the mixture and the components included in the dry air. We can state, only roughly, that the range of validity of the model is for pressures up to 30 MPa. Extrapolation of the model up to 100 MPa should be possible, but the user should be quite careful to ensure reasonable extrapolation. Experimental data (Gernert and Span, 2016) exist at temperatures as high as 1000 K for the mixture of carbon dioxide and water. Maximum measured temperature of the experimental data are much lower for other binary pairs.

4.2. Derived properties

4.2.1. Humidity ratio

The humidity ratio W is defined as the ratio of the mass of water in the mixture to the mass of dry air, or

$$W \equiv \frac{m_{\rm H_2O}}{m_{\rm da}} = \frac{M_{\rm H_2O}}{M_{\rm da}}\frac{x_{\rm H_2O}}{1 - x_{\rm H_2O}}. \tag{17}$$

If the humidity ratio W is known, the water mole fraction $x_{\rm H_2O}$ can be obtained from

$$x_{\rm H_2O} = \frac{W\dfrac{M_{\rm da}}{M_{\rm H_2O}}}{1 + W\dfrac{M_{\rm da}}{M_{\rm H_2O}}}. \tag{18}$$

4.2.2. Relative humidity

There are a number of different definitions for the relative humidity of humid air available in the literature; Lovell-Smith *et al.* (2016) covers the definitions in use. A thermodynamically rigorous definition of the relative humidity is that it is the ratio of the fugacity of the water vapor in the mixture to the fugacity of the water in a humid air mixture in equilibrium with the first droplet of liquid (the definition of the dew point).

For consistency with the existing literature and standards for humidity measurement, we define the relative humidity as the ratio (all at the same temperature and pressure) of the mole fraction of water in the bulk gaseous phase to the mole fraction of water in equilibrium with the first frost or liquid droplet. As discussed below, an iterative solution is required to obtain the mole fraction of water in the vapor phase at saturation. Thus we can define the relative humidity ϕ as

$$\phi \equiv \frac{x_{\mathrm{H_2O}}}{x''_{\mathrm{H_2O,sat}}(T,p)} \tag{19}$$

If the dry-bulb temperature T and pressure p are known, $x''_{\mathrm{H_2O,sat}}$ can be obtained through the use of the methods presented below, and $x_{\mathrm{H_2O}}$ can be obtained from Eq. 19 for the given relative humidity ϕ.

4.2.3. Dew point

The dew point of humid air is the temperature where the first droplet of liquid water (or first crystal of ice) condenses out of a humid air mixture as it is cooled at constant pressure and water content. The algorithm used to obtain the dew-point temperature and/or molar composition is presented in section 5.

4.2.4. Wet-bulb temperature

The World Meteorological Organization (WMO) defines the thermodynamic wet-bulb temperature by: "The thermodynamic wet-bulb temperature of moist air at pressure p, temperature T and mixing ratio r is the temperature T_w attained by the moist air when brought adiabatically to saturation at pressure p by the evaporation into the moist air of liquid water at pressure p and temperature T_w and containing the amount of dissolved air corresponding to equilibrium with saturated air of the same pressure and temperature" (Jarraud, 2008, Eq. 4.A.18). A similar definition is available for the same process with an ice phase, yielding the ice-bulb temperature.

From the analysis of the adiabatic saturator, it can be shown (see Herrmann *et al.* (2009a) and the supplemental material of this paper) that the wet-bulb temperature can be defined by the equality

$$h + \left(\frac{1-x_{\mathrm{H_2O}}}{1-x''_{\mathrm{H_2O}}} - 1\right) h_{\mathrm{H_2O},0} = \left(\frac{1-x_{\mathrm{H_2O}}}{1-x''_{\mathrm{H_2O}}}\right) h'' \tag{20}$$

where: h is the humid air specific enthalpy of humid air evaluated at the dry-bulb temperature T_{db} (the usual thermodynamic temperature of the given humid-air sample), the absolute pressure p, and the water mole fraction $x_{\mathrm{H_2O}}$; h'' is the humid air specific enthalpy of the saturated humid air in equilibrium with either ice or water, evaluated at the wet-bulb temperature T_{wb}, the total pressure p, and the water mole fraction at saturation $x''_{\mathrm{H_2O}}$; and $h_{\mathrm{H_2O},0}$ is the enthalpy of either pure water or ice, evaluated at the wet-bulb temperature T_{wb}. The derivation of the equality in Eq. 20 can be found in the supplemental material. The equation in Eq. 20 must in general be solved iteratively, as described below.

4.2.5. Enhancement factor

The enhancement factor is defined as the ratio of the saturated partial pressure of water in humid air to the saturation pressure of pure water at the given temperature. The enhancement factor explicitly appears in many psychrometric models, while it is exclusively an output in this model (and can be calculated from the saturation routines). The enhancement factor f_{e} (normally given the symbol f, but f is primarily used for fugacity in this work) is given by

$$f_{\mathrm{e}} = \frac{x''_{\mathrm{H_2O,sat}}\,p}{p_{\mathrm{sat,H_2O},0}} \tag{21}$$

5. Phase equilibria routines

There are two general types of phase equilibrium calculations to be considered in psychrometric routines:

- For a specified vapor phase composition, determine the dew-point temperature where the humid air is in equilibrium with liquid (or ice). This corresponds to the intersection of a horizontal line and the saturation curve on a psychrometric chart.
- For a specified dry-bulb temperature, determine the vapor-phase composition that will yield humid air in equilibrium with liquid (or ice). This corresponds to the intersection of a vertical line and the saturation curve on a psychrometric chart.

Figure 2 gives a graphical representation of the two types of phase equilibria routines that must be developed for psychrometric calculations.

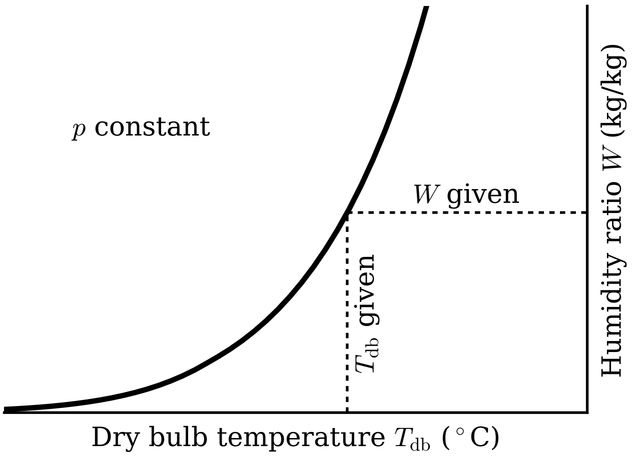

Figure 2: Schematic demonstrating the two families of phase equilibrium calculations needed for humid air routines. The solid line represent the dew point curve.

Another challenge with psychrometric properties is the potential for the formation of air hydrates (molecules of gas trapped in a matrix of water molecules) at high pressures. The experimental data and modeling results from the literature (Mohammadi and Richon, 2010; Mohammadi et al., 2003; Yasuda et al., 2013; Vinš et al., 2016, 2017; Jäger et al., 2016) suggest that air hydrates could form at pressures as low as approximately 10 MPa. In spite of the identified potential for the formation of hydrates, hydrate formation is *explicitly* not considered in this model formulation. Several research groups around the world are actively involved in modeling the formation of air hydrates, and once their modeling work is complete, their models could be integrated into the psychrometric property routines presented here.

In the case of solid water (ice) in equilibrium with humid air vapor, a simplifying assumption is that the ice is pure, and has no dissolved gases. In reality, there will be some gas molecules that will be found in the ice matrix, but they can be neglected. The essentially zero solubility of gases in ice is the reason that freeze-evacuate-thaw cycling is used to *remove* dissolved gases from liquids.

When a property of humid air is desired as a function of temperature and pressure, it is necessary to first determine whether the coexisting saturation water phase corresponds to a liquid or solid. This determination can be made based on the melting curve of normal water from Wagner et al. (2011), where the melting pressure is expressed as an explicit function of the temperature. The melting pressure is evaluated from the melting curve for a given temperature; if the pressure is above the melting pressure, it is liquid, and if below, it is solid. We explicitly only consider the Ih phase of ice, which simplifies the phase determination (because the complete melting curve is multi-valued for temperatures below 273.16 K, and the Ih melting line is monotonic).

Algorithm:

1. If $T > 273.16$ K, pure ice cannot exist below pressures of approximately 630 MPa (according to the ice phase V melting line (Wagner et al., 2011)), therefore solid-vapor equilibrium is not possible and liquid-vapor equilibrium must be considered.
2. Otherwise, either solid-vapor or liquid-vapor equilibria are possible. In this case, carry out both phase equilibrium calculations, and keep the equilibrium that results in the lower chemical potential of water vapor in the vapor phase. This corresponds to the phase configuration that is thermodynamically preferred.

5.1. Liquid-vapor equilibrium evaluation

In a classical mixture dew point calculation (for instance in natural gas mixtures), the vapor-phase composition is fully specified, and then one of either the temperature or pressure is specified and the other is obtained iteratively.

While the conventional dew point calculation is required for psychrometry, it is also necessary to be able to efficiently carry out the backwards evaluation, where the dew-point temperature is known, and the composition of the vapor phase must be obtained through iteration - in particular, the water mole fraction of the vapor phase must be determined for the specified temperature and pressure at saturation.

The algorithm required for the determination of the vapor-phase composition for a given dew point state for mixtures with arbitrary dry air composition is somewhat more complex than the conventional dew point calculation, and to our knowledge has not been published before. An implementation of this inverse calculation for air of fixed air composition is given in the open-source TEOS-10 model (Feistel et al., 2010).

In the calculations in this section, the relative composition of the dry air (in the vapor phase) is held constant, as is the absolute pressure. In the liquid phase, there is no constraint on the relative solubility between dry air constituents.

5.1.1. Temperature specified

In the case of a four-component dry air mixture, the humid air mixture has $N = 5$ components. The independent variables are $N-1$ compositions of the dry air constituents in the liquid phase (x'_1 to x'_{N-1}) and the water mole fraction in the vapor phase $x''_{\mathrm{H_2O}}$. In vector form, the independent variables can be given by

$$\boldsymbol{X} = \begin{pmatrix} x'_1 \\ x'_2 \\ \vdots \\ x'_{N-1} \\ x''_{\mathrm{H_2O}} \end{pmatrix} \tag{22}$$

One of the challenges of this formulation has to do with the composition derivatives. In the mixture model and composition derivatives developed by Gernert and coworkers (Gernert et al., 2014; Gernert and Span, 2016), the last component in the mixture is a dependent variable, and is obtained from the summation of the preceding $N-1$ mole fractions as

$$x_N = 1 - \sum_{i=1}^{N-1} x_i. \tag{23}$$

In this formulation, it is not possible to take derivatives of any property with respect to x_N. It is necessary to take derivatives with respect to the mole fractions of all of the dry air constituents in the liquid phase (x'_1 to x'_{N-1}), as well as the mole fraction of water in the vapor phase $x''_{\mathrm{H_2O}}$. In the liquid phase, the water mole fraction must be an independent variable, and in the vapor phase, the water mole fraction must be a dependent variable.

The resolution to this problem is to sort the arrays of components and compositions differently for the liquid and vapor phases. Therefore, we write the liquid composition array as

$$\boldsymbol{x}' = [x_{\mathrm{N_2}}, x_{\mathrm{O_2}}, x_{\mathrm{Ar}}, x_{\mathrm{CO_2}}, x_{\mathrm{H_2O}}] \tag{24}$$

and the vapor composition array as

$$\boldsymbol{x}'' = [x_{\mathrm{H_2O}}, x_{\mathrm{N_2}}, x_{\mathrm{O_2}}, x_{\mathrm{Ar}}, x_{\mathrm{CO_2}}]. \tag{25}$$

In this way we can take the necessary derivatives; the only challenge is associated with some additional bookkeeping in the code to ensure that the indices in the arrays are consistently and correctly used.

The residual functions to be driven to zero are N equalities of fugacities (on a natural logarithm basis) for all the components (dry air and water) given by equations of the form

$$F_i = \ln(f'_i) - \ln(f''_i) \tag{26}$$

where, as described above, the implementer must be careful to ensure that the correct indices are being used. The Jacobian matrix is given by

$$\mathbf{J} = \begin{bmatrix} \left(\frac{\partial F_1}{\partial x'_1}\right)_{x'_j} & \cdots & \left(\frac{\partial F_1}{\partial x'_{N-1}}\right)_{x'_j} & \left(\frac{\partial F_1}{\partial x''_{\mathrm{H_2O}}}\right)_{x''_j} \\ \left(\frac{\partial F_2}{\partial x'_1}\right)_{x'_j} & \cdots & \left(\frac{\partial F_2}{\partial x'_{N-1}}\right)_{x'_j} & \left(\frac{\partial F_2}{\partial x''_{\mathrm{H_2O}}}\right)_{x''_j} \\ \vdots & \ddots & \vdots & \vdots \\ \left(\frac{\partial F_N}{\partial x'_1}\right)_{x'_j} & \cdots & \left(\frac{\partial F_N}{\partial x'_{N-1}}\right)_{x'_j} & \left(\frac{\partial F_N}{\partial x''_{\mathrm{H_2O}}}\right)_{x''_j} \end{bmatrix}, \tag{27}$$

where all partial derivatives are taken at constant temperature, pressure, and all other compositions held constant.

Algorithm:

1. The first guess for the water mole fraction is given by $x''_{\mathrm{H_2O},0} = p_{\mathrm{sat,H_2O},0}(T)/p$ (here assuming an enhancement factor of unity).
2. For a given water mole fraction $x''_{\mathrm{H_2O}}$ in the vapor phase, evaluate the vapor-phase composition through the use of Eqs. 2 to 6.
3. In the first iteration, estimate the liquid composition through the use of Henry's law (see section 5.1.3). In subsequent iterations, skip this step.
4. Calculate $\rho(T, p)$ for the liquid and vapor phases. In the first iteration, estimate the liquid density as being pure saturated liquid water at the specified temperature, and the vapor phase as being a mixture of ideal gases. Cache calculated densities as initial estimates for the next iteration. In subsequent iterations, use the cached densities as guess densities.
5. Construct the residual vector $\boldsymbol{r}$ with entries given from Eq. 26 and the Jacobian matrix from Eq. 27. All necessary derivatives are explained in Gernert *et al.* (2014; 2016); see especially the supplemental material in Gernert *et al.* (2014).
6. Solve $\mathbf{J}\Delta\boldsymbol{X} = -\boldsymbol{r}$ for $\Delta\boldsymbol{X}$ and update the vector $\boldsymbol{X}$ with $\boldsymbol{X}_{\mathrm{new}} = \boldsymbol{X}_{\mathrm{old}} + \Delta\boldsymbol{X}$. Update the liquid and vapor compositions.
7. Return to step # 2 until convergence is reached (when the maximal mole fraction change is less than the acceptable tolerance).

Figure 3 shows the water mole fractions in the vapor phase at equilibrium. As the temperature approaches the saturation temperature of pure water at the given pressure, the water mole fraction at equilibrium approaches unity; the vapor phase at equilibrium becomes pure water.

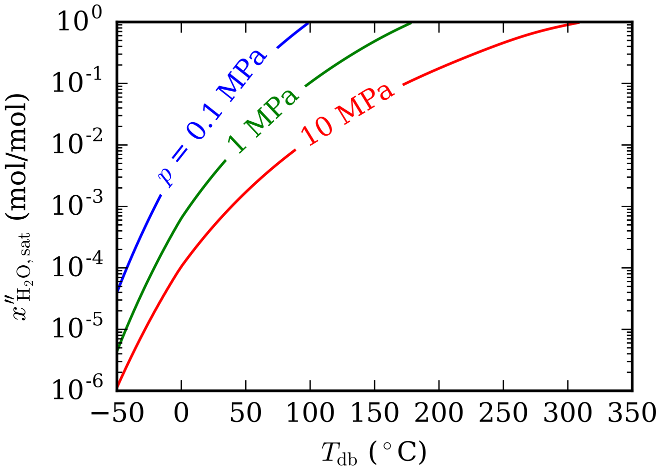

Figure 3: Water mole fractions in vapor phase for humid air in equilibrium with incipient water or ice phase for a range of pressures. Below 0.01 °C, the solid-vapor equilibrium routines are employed.

5.1.2. Vapor-phase composition specified

In the calculation for a dew point, the pressure and $x''_{\mathrm{H_2O}}$ are given, and it is necessary to obtain the dry-bulb temperature T_{db} at saturation. The numerical analysis required to evaluate a dew point is quite straightforward. The algorithm used is nearly identical to the algorithm for $x''_{\mathrm{H_2O}}$ except that the variable $x''_{\mathrm{H_2O}}$ is replaced with T in the matrix of independent variables and also in the Jacobian matrix. Thus the vector of independent variables is given by

$$\boldsymbol{X} = \begin{pmatrix} x'_1 \\ x'_2 \\ \vdots \\ x'_{N-1} \\ T \end{pmatrix} \tag{28}$$

and the Jacobian matrix is given by

$$\mathbf{J} = \begin{bmatrix} \left(\dfrac{\partial F_1}{\partial x'_1}\right)_{T,x'_j} & \cdots & \left(\dfrac{\partial F_1}{\partial x'_{N-1}}\right)_{T,x'_j} & \left(\dfrac{\partial F_1}{\partial T}\right)_{\boldsymbol{x}} \\ \left(\dfrac{\partial F_2}{\partial x'_1}\right)_{T,x'_j} & \cdots & \left(\dfrac{\partial F_2}{\partial x'_{N-1}}\right)_{T,x'_j} & \left(\dfrac{\partial F_2}{\partial T}\right)_{\boldsymbol{x}} \\ \vdots & \ddots & \vdots & \vdots \\ \left(\dfrac{\partial F_N}{\partial x'_1}\right)_{T,x'_j} & \cdots & \left(\dfrac{\partial F_N}{\partial x'_{N-1}}\right)_{T,x'_j} & \left(\dfrac{\partial F_N}{\partial T}\right)_{\boldsymbol{x}} \end{bmatrix}, \tag{29}$$

where all partial derivatives are taken at constant pressure and the same residual functions are used as in Eq. 26.

The initialization and estimation of the liquid-phase composition proceeds in the same fashion as the evaluation of the vapor-phase composition at the dew point. We obtain a first guess for the dew-point temperature by assuming a unity enhancement factor, which yields the partial pressure of water from $p_{\mathrm{sat,H_2O,0}} = x''_{\mathrm{H_2O}} \cdot p$. The vapor-pressure curve can be inverted (in some cases, like the IAPWS-IF97 industrial formulation for water (Wagner and Kretzschmar, 2007), without iteration), to yield the estimated dew-point temperature from

$$T_{\mathrm{db,est}} = T_{\mathrm{sat,H_2O,0}}(x''_{\mathrm{H_2O}}p) \tag{30}$$

by the algorithm described above.

Figure 4 shows the error in the initial estimate of the dew-point temperature from this scheme. The water saturation composition was calculated by the algorithm described above to obtain $x''_{\mathrm{H_2O}}$ for the given pressure, and $T_{\mathrm{sat,H_2O,0}}$ is obtained from the equation of state of Wagner and Pruß(2002). While the errors are up to approximately 9 K, this accuracy is sufficient to yield convergence for pressures from 0.1 MPa to 10 MPa. The liquid-phase composition is then estimated based on Henry's law for the given vapor composition, pressure, and estimated temperature.

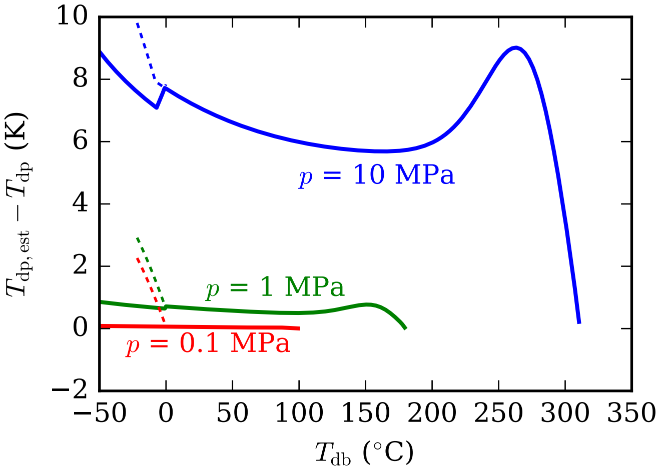

Figure 4: Error in the estimation scheme for the first guess of dew-point or frost-point temperature as a function of dry-bulb temperature for three pressures as compared with the full phase equilibrium calculation for the dewpoint. The dashed lines show the non-thermodynamically-preferred incipient phase, in this case a liquid water phase.

5.1.3. *Liquid-phase composition estimates*

One of the challenges in the evaluation of the dew point is that the conventional means used to estimate the composition of the incipient liquid phase are significantly incorrect. Most commonly, Wilson's method (1968) is used to predict the liquid-phase composition. Wilson's equation yields an explicit solution for the liquid-phase composition given the vapor-phase composition and the temperature and pressure. While Wilson's method was originally developed for hydrocarbon mixtures, it remains the default estimation scheme for a wide range of mixtures due to a lack of better alternatives of equivalent simplicity. Less accurate initial estimates for the liquid-phase composition hinder the convergence of the numerical solvers commonly applied to dew point calculations. More accurate initial estimates for the liquid-phase composition can be obtained through the use of Henry's law, because the liquid phase is very nearly pure water. Henry's law constants for the solubility of component i in pure water are defined as the ratio of the pure component's fugacity in the vapor phase to the mole fraction of that constituent in the liquid phase in the infinite-dilution limit. Mathematically, this can be expressed as

$$k_{\mathrm{H}} \equiv \lim_{x'_i \to 0} \frac{f_i}{x'_i}, \tag{31}$$

and by dropping the limit, the solute mole fraction can be estimated from

$$x'_i = \frac{f_i}{k_{\mathrm{H}}}, \tag{32}$$

where the fugacity f_i and the Henry's law constant k_{H} are both given in the same unit of pressure. If the vapor phase is furthermore assumed to be a mixture of ideal gases, then the solute mole fraction can be given by

$$x'_i = \frac{x''_i p}{k_{\mathrm{H}}}, \tag{33}$$

because the fugacity of a component in an ideal gas mixture is simply its partial pressure. In this case, we are only looking to obtain a reasonably good estimate of the water-phase composition, and the use of the ideal gas assumption for the vapor phase is entirely appropriate.

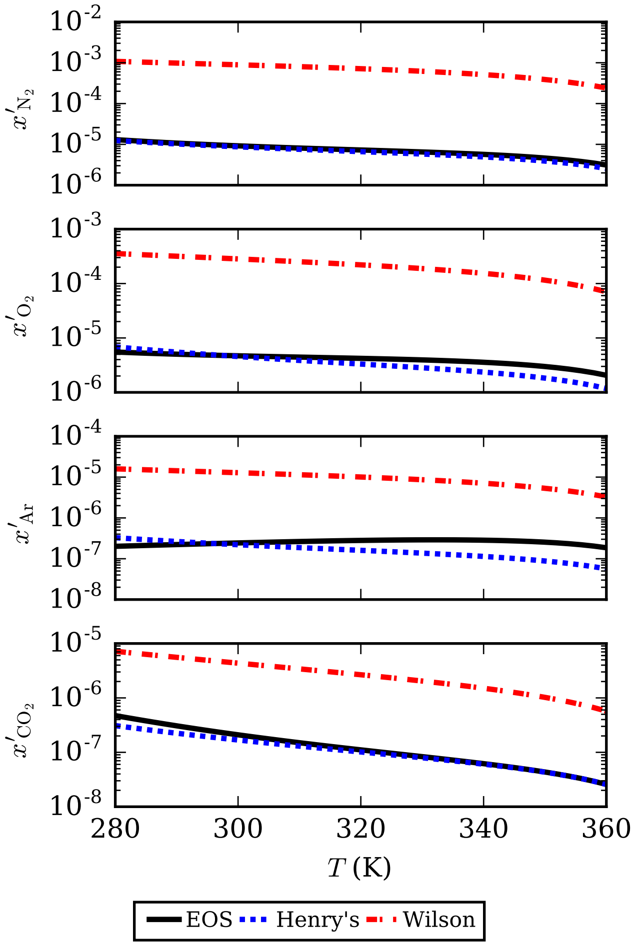

Figure 5: Liquid-phase compositions for dew points calculated from the full mixture model, Henry's law, and Wilson's method estimation schemes at 101.325 kPa (1 atmosphere). At each temperature, a dew-point calculation is carried out to obtain the vapor-phase composition and the incipient liquid-phase composition.

In the work of Fernández-Prini *et al.* (2003), the Henry's law constants for the components of dry air have been fitted to the form proposed by Harvey (1996) in terms of reduced temperatures:

$$\ln\left(\frac{k_{\rm H}}{p_{\rm sat,H_2O,0}}\right) = \frac{A}{T_{\rm R}} + \frac{B(\tau^*)^{0.355}}{T_{\rm R}} + C\cdot(T_{\rm R})^{-0.41}\exp\tau^*, \tag{34}$$

where the reduced temperature $T_{\rm R}$ is given by $T_{\rm R} = T/T_{\rm c}$, $T_{\rm c}$ is the critical temperature of pure water (647.096 K), τ^* is given by $\tau^* = 1 - T_{\rm R}$, and $p_{\rm sat,H_2O,0}$ is the saturation pressure of pure water at temperature T. Through the use of this form, the Henry's law constants are evaluated for the components of dry air, and Eq. 33 is used to estimate the liquid-phase composition, with the assumption that the solubility of one air constituent has no impact on the solubility of another air constituent. The water mole fraction in the liquid phase then becomes simply

$$x'_N = x'_{\rm H_2O} = 1 - \sum_{i=1}^{N-1} x'_i. \tag{35}$$

Figure 5 shows the comparison of the liquid-phase compositions as calculated with the entire mixture model presented in section 5.1.1 as well as the liquid-phase compositions calculated by Henry's law constants at 101.325 kPa. While the quantitative agreement is not excellent, the qualitative agreement is entirely sufficient to use this model as an initial guess for the Newton-Raphson solver that is used to solve for the saturation state.

5.2. Solid-vapor equilibrium evaluation

The equilibrium of pure ice and humid air vapor is achieved when the chemical potential of water vapor in humid air equals that of the chemical potential of the pure ice at the same temperature and pressure. The definition of the chemical potential of the i-th component in a mixture (see for instance Jäger (2015, Eq. 3.14)) is

$$\mu_i = \left(\frac{\partial[n\cdot g(T,p,\boldsymbol{x})]}{\partial n_i}\right)_{T,p,n_j}, \tag{36}$$

and because the molar Gibbs energy of a pure fluid g is not a function of the number of moles n_i in a one-component mixture in which $n_i = n$, $\mu_{i,\rm ice} = g_{\rm ice}$.

In the vapor phase, for a given temperature and pressure, the chemical potential of water vapor can be evaluated from the mixture model, the details of which are described in the GERG models (Kunz et al., 2007; Kunz and Wagner, 2012).

5.2.1. Vapor-phase composition specified

If the composition of the vapor phase is known, the frost-point temperature must be obtained. For this case, the residual function for the frost-point temperature to be driven to zero is given by

$$F(T_{\rm fp}) = g_{\rm ice}(T_{\rm fp},p) - \mu_{\rm H_2O}(T_{\rm fp},p). \tag{37}$$

As in the case of vapor-liquid equilibrium, the first guess for the frost-point temperature is that the enhancement factor is one, and therefore, the estimated frost-point temperature is obtained from

$$T_{\rm fp,est} = T_{\rm ice,subl}(x''_{\rm H_2O}\cdot p) \tag{38}$$

where the sublimation curve of Wagner *et al.* (2011) is inverted numerically to evaluate the $T_{\rm ice,subl}$ function for the partial pressure of water vapor given by $x''_{\rm H_2O}\cdot p$.

5.2.2. Temperature specified

If the frost-point temperature is specified, and the water vapor composition is to be obtained, the residual to be driven to zero is given by

$$F(x''_{\mathrm{H_2O}}) = g_{\mathrm{ice}}(T_{\mathrm{fp}}, p) - \mu_{\mathrm{H_2O}}(T_{\mathrm{fp}}, p, x''_{\mathrm{H_2O}}). \tag{39}$$

The first guess for the composition of the vapor phase is again that the enhancement factor is one, and therefore that the water mole fraction can be estimated from

$$x''_{\mathrm{H_2O,est}} = \frac{p_{\mathrm{ice,subl}}(T_{\mathrm{fp}})}{p}, \tag{40}$$

where the sublimation curve of Wagner *et al.* (2011) is used to evaluate the $p_{\mathrm{ice,subl}}$ function for the frost-point temperature T_{fp}.

6. Flash routines

Dew and bubble-point calculations form but a subset of the types of mixture calculations that are possible. Another type of calculation that is commonly required is that of flash calculations. In flash calculations, variables other than the natural variables of the mixture model (here τ, δ, and $\boldsymbol{x}$) are transformed into the natural variables of the mixture model.

6.1. Density

If dry-bulb temperature, pressure, and density are known (for instance when constructing psychrometric charts), the mole fraction of water $x_{\mathrm{H_2O}}$ must be obtained through the use of an iterative solver, which in this case could be a bounded solver like Brent's method (Brent, 1973) as it is known that the mole fraction of water is between zero and $x''_{\mathrm{H_2O,sat}}(T)$ inclusive. The residual function to be driven to zero by the numerical solver could be given by

$$F(x_{\mathrm{H_2O}}) = p(T, \rho, x_{\mathrm{H_2O}})/p_{\mathrm{given}} - 1. \tag{41}$$

If density, pressure, and the mole fraction of water are known, the dry-bulb temperature T_{db} must be determined. In the gas phase, it is known that the compressibility factor Z is very nearly unity. Thus, an initial guess for the temperature is $T_{\mathrm{guess}} = p/(\rho R)$ (for $Z = 1$), and the residual function could be given by

$$F(T) = p(T, \rho, x_{\mathrm{H_2O}})/p_{\mathrm{given}} - 1, \tag{42}$$

which can be reliably solved with a secant solver.

6.2. Wet-bulb temperature

By definition, the thermodynamic wet-bulb temperature T_{wb} must be less than the dry-bulb temperature T_{db}, and both temperatures are equal when the air is saturated (equivalently, when $\phi = 1$, $x_{\mathrm{H_2O}} = x''_{\mathrm{H_2O}}$, or $W = W''_{\mathrm{wb}}$).

There are a few common evaluations that involve the use of wet-bulb temperature (each for total pressure imposed):

- Wet-bulb and dry-bulb temperatures are known, $x_{\mathrm{H_2O}}$ is desired (the classic psychrometric calculation).
- Dry-bulb temperature and $x_{\mathrm{H_2O}}$ are known, wet-bulb temperature is desired.
- Wet-bulb temperature and $x_{\mathrm{H_2O}}$ are known, dry-bulb temperature is desired (for determining the wet-bulb temperature of dry air).

For each evaluation, the algorithm involves the evaluation of saturated air properties in combination with humid air properties. Here we describe each algorithm in detail.

6.2.1. $x_{\mathrm{H_2O}}$ from T_{db} and T_{wb}

For the given wet-bulb temperature T_{wb} and total pressure p, the pure water (or ice) enthalpy $h_{\mathrm{H_2O,0}}$ is evaluated as described in section 3.2. The phase equilibrium routines of section 5 are used to obtain $x''_{\mathrm{H_2O}}$ (and subsequently h'') for the given T_{wb}. Therefore, the unknown variables in Eq. 20 are h and $x_{\mathrm{H_2O}}$. The water mole fraction $x_{\mathrm{H_2O}}$ is known to be between zero and the saturation water vapor fraction obtained from $x''_{\mathrm{H_2O}}(T_{\mathrm{wb}})$. Therefore, a bounded solver, here Brent's method with quadratic updating (Brent, 1973), is used to solve for the water mole fraction $x_{\mathrm{H_2O}}$ that satisfies Eq. 20.

6.2.2. T_{wb} from T_{db} and $x_{\mathrm{H_2O}}$

For the given dry-bulb temperature T_{db}, total pressure p, and water mole fraction $x_{\mathrm{H_2O}}$, the humid air enthalpy h is obtained. The unknowns in Eq. 20 are then $x''_{\mathrm{H_2O}}$, h'', and $h_{\mathrm{H_2O,0}}$. The wet-bulb temperature T_{wb} is known to be less than the dry-bulb temperature and greater than a very low temperature (here 100 K); a bounded solver, here Brent's method with quadratic updating (Brent, 1973), is used to solve for the wet-bulb temperature T_{wb} that satisfies Eq. 20. At each step in the iteration for T_{wb}, the pure water/ice enthalpy $h_{\mathrm{H_2O,0}}$ is evaluated as described in section 3.2, and the phase equilibrium routines of section 5 are used to obtain $x''_{\mathrm{H_2O}}$ and subsequently h'' for the given T_{wb}.

6.2.3. T_{db} from $x_{\mathrm{H_2O}}$ and T_{wb}

For the given wet-bulb temperature T_{wb}, the pure water/ice enthalpy $h_{\mathrm{H_2O,0}}$ is evaluated as described in section 3.2. The phase equilibrium routines of section 5 are used to obtain $x''_{\mathrm{H_2O}}$ and subsequently h'' for the given T_{wb}. Therefore, the only remaining variable in Eq. 20 is h. The dry-bulb temperature T_{db} is known to be above the wet-bulb temperature T_{wb} and below the saturation temperature of pure water or ice at the total pressure p. Therefore, a bounded solver, here Brent's method with quadratic updating (Brent, 1973), is used to solve for the dry-bulb temperature T_{db} that satisfies Eq. 20. At high values of T_{wb}, it is sometimes impossible to solve for T_{db} because the dry-bulb temperature is above the saturation temperature of pure water.

7. Implementation and Results

7.1. Implementation

The algorithms described here have been implemented into a C++ library, with native wrappers available for Python through the use of the `pybind11` [3] package. Wrappers for additional high-level programming languages can be readily constructed through the use of the `SWIG` (Simplified Wrapper and Interface Generator) package.

The source code of this library is provided as supplemental material as well as instructions for compiling standalone examples and the wrappers.

7.2. Psychrometric chart

The algorithms presented above can be used to construct the psychrometric chart, as seen in Figure 6. This chart represents the links between the thermodynamic variables for a humid air mixture. In this variant of the psychrometric chart, we plot the lines of constant relative humidity, lines of constant wet-bulb temperature, and the lines of constant specific volume (on a per-kg-dry-air basis). The density (on a per-kg-humid-air basis) can be obtained from the specific volume per kilogram dry air from

$$\rho = \frac{W+1}{v_{\rm da}M_{\rm ha}} \tag{43}$$

In this psychrometric chart we have used orthogonal axes for ease of plotting, while the ASHRAE standard psychrometric charts have slightly non-orthogonal axes (ASHRAE, 2001). The lines of constant relative humidity were constructed by first determining the saturation ($\phi = 1$) humidity ratio and multiplying by the relative humidity (and subsequently converting from water mole fraction to humidity ratio). Lines of constant dry-air-specific volume were constructed by first interpolating the saturation curve to determine the value of $x_{\rm H_2O}$ corresponding to this specific volume, then evaluating $T(p, v_{\rm da}, x_{\rm H_2O})$ between the saturation water mole fraction $x''_{\rm H_2O,sat}(v_{\rm da})$ and dry air ($x_{\rm H_2O} = 0$).

Conclusions

In this work, we have developed the necessary algorithms to carry out the most important psychrometric calculations for mixtures modeled with the multi-fluid GERG formulation. This framework can be applied to mixtures of arbitrary air composition, and can be applied to the construction of psychrometric charts, among other calculations. A C++-based implementation of the algorithms is presented in the supplemental material.

Acknowledgments

This paper extends the analysis presented in a paper at the 2016 Purdue University Refrigeration conference (Bell et al., 2016).

ASHRAE, 2001. Fundamentals. American Society of Heating, Refrigerating and Air Conditioning Engineers (ASHRAE).

Bell, I. H., Lemmon, E. W., Harvey, A. H., 2016. Psychrometric Properties of Humid Air from Multi-Fluid Helmholtz-Energy-Explicit Models. In: 16th International Refrigeration and Air Conditioning Conference at Purdue, July 11-14, 2016. p. 2288.

Brent, R., 1973. Algorithms for Minimization without Derivatives. Prentice-Hall, Ch. 4.

Feistel, R., Wagner, W., 2006. A New Equation of State for H_2O Ice Ih. J. Phys. Chem. Ref. Data 35 (2), 1021–1047.

Feistel, R., Wright, D. G., Jackett, D. R., Miyagawa, K., Reissmann, J. H., Wagner, W., Overhoff, U., Guder, C., Feistel, A., Marion, G. M., 2010. Numerical implementation and oceanographic application of the thermodynamic potentials of liquid water, water vapour, ice, seawater and humid air – part 1: Background and equations. Ocean Science 6 (3), 633–677.
URL `http://www.ocean-sci.net/6/633/2010/`

Fernández-Prini, R., Alvarez, J. L., Harvey, A. H., 2003. Henry's Constants and Vapor-Liquid Distribution Constants for Gaseous Solutes in H_2O and D_2O at High Temperatures. J. Phys. Chem. Ref. Data 32 (2), 903–916.

Gernert, J., Jäger, A., Span, R., 2014. Calculation of phase equilibria for multi-component mixtures using highly accurate Helmholtz energy equations of state. Fluid Phase Equilib. 375, 209–218.

Gernert, J., Span, R., 2016. EOS-CG: A Helmholtz energy mixture model for humid gases and CCS mixtures. J. Chem. Thermodyn. 93, 274–293.

Harvey, A. H., 1996. Semiempirical correlation for Henry's constants over large temperature ranges. AIChE J. 42 (5), 1491–1494.

Herrmann, S., Kretzschmar, H.-J., Gatley, D. P., 2009a. Thermodynamic Properties of Real Moist Air, Dry Air, Steam, Water, and Ice (RP-1485). HVAC&R Research 15 (5), 961–986.

Herrmann, S., Kretzschmar, H.-J., Teske, V., Vogel, E., Ulbig, P., Span, R., Gatley, D., 2009b. Berechnung der thermodynamischen Zustandsgrö*β*en und Transporteigenschaften von feuchter Luft für energietechnische Prozessmodellierungen (Determination of Thermodynamic and Transport Properties of Humid Air for Power-Cycle Calculations). Tech. rep., Physikalisch-Technische Bundesanstalt (PTB).

Jäger, A., 2015. Complex Phase Equilibria of Gas Hydrates and other Solid and Fluid Phases Modeled With Highly Accurate Equations of State. Ph.D. thesis, Ruhr-Universität Bochum.

Jäger, A., Vinš, V., Span, R., Hrubý, J., 2016. Model for gas hydrates applied to CCS systems part III. Results and implementation in TREND 2.0. Fluid Phase Equilib. 429, 55–66.

Jarraud, M., 2008. Guide to meteorological instruments and methods of observation (wmo-no. 8). World Meteorological Organisation: Geneva, Switzerland.

Kunz, O., Klimeck, R., Wagner, W., Jaeschke, M., 2007. The GERG-2004 Wide-Range Equation of State for Natural Gases and Other Mixtures. VDI Verlag GmbH.

Kunz, O., Wagner, W., 2012. The GERG-2008 Wide-Range Equation of State for Natural Gases and Other Mixtures: An Expansion of GERG-2004. J. Chem. Eng. Data 57, 3032–3091.

Lovell-Smith, J. W., Feistel, R., Harvey, A. H., Hellmuth, O., Bell, S. A., Heinonen, M., Cooper, J. R., 2016. Metrological challenges for measurements of key climatological observables. Part 4: atmospheric relative humidity. Metrologia 53 (1), R40–R59.

Mohammadi, A. H., Richon, D., 2010. Ice–Clathrate Hydrate–Gas Phase Equilibria for Air, Oxygen, Nitrogen, Carbon Monoxide, Methane, or Ethane + Water System. Ind. Eng. Chem. Res. 49, 3976–3979.

Mohammadi, A. H., Tohidi, B., Burgass, R. W., 2003. Equilibrium Data and Thermodynamic Modeling of Nitrogen, Oxygen, and Air Clathrate Hydrates. J. Chem. Eng. Data 48, 612–616.

---

[3] `https://github.com/pybind/pybind11`

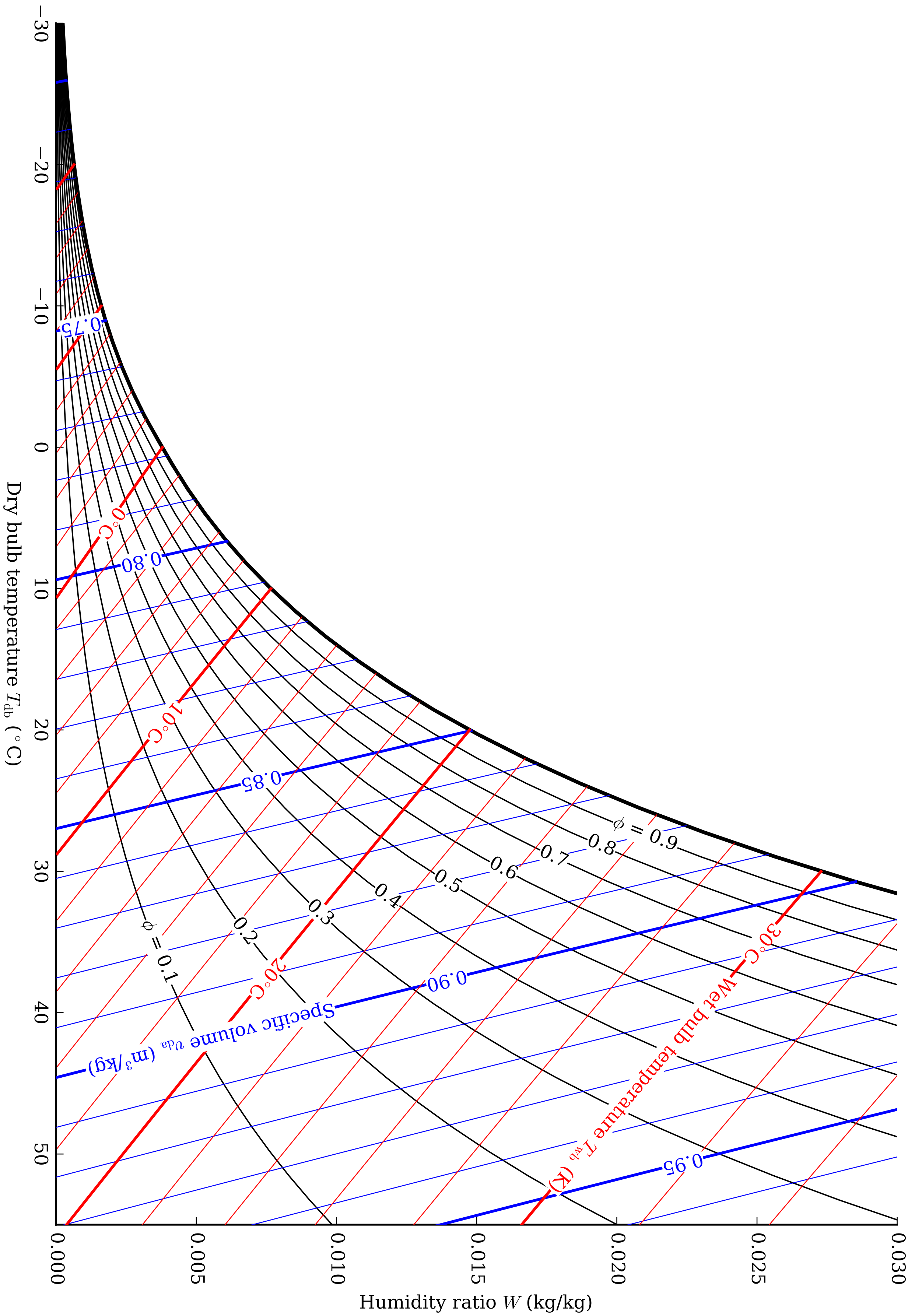

Figure 6: Psychrometric chart at 101.325 kPa (1 atmosphere) as in the work of Zhang and Pate (1988)

Nelson, H. F., Sauer, H. J., 2002. Formulation of High-Temperature Properties for Moist Air. HVAC&R Research 8 (3), 311–334.

Picard, A., Davis, R., Gläser, M., Fujii, K., 2008. Revised formula for the density of moist air (CIPM-2007). Metrologia 45 (2), 149–155.

Schmidt, R., Wagner, W., 1985. A New Form of the Equation of State for Pure Substances and its Application to Oxygen. Fluid Phase Equilib. 19 (3), 175–200.

Shallcross, D. C., 2005. Preparation of psychrometric charts for water vapour in Martian atmosphere. Int. J. Heat Mass Tran. 48 (9), 1785–1796.

Span, R., 2000. Multiparameter Equations of State - An Accurate Source of Thermodynamic Property Data. Springer.

Span, R., Lemmon, E. W., Jacobsen, R. T., Wagner, W., Yokozeki, A., 2000. A Reference Equation of State for the Thermodynamic Properties of Nitrogen for Temperatures from 63.151 to 1000 K and Pressures to 2200 MPa. J. Phys. Chem. Ref. Data 29, 1361–1433.

Span, R., Wagner, W., 1996. A New Equation of State for Carbon Dioxide Covering the Fluid Region from the Triple Point Temperature to 1100 K at Pressures up to 800 MPa. J. Phys. Chem. Ref. Data 25, 1509–1596.

Tegeler, C., Span, R., Wagner, W., 1999. A New Equation of State for Argon Covering the Fluid Region for Temperatures From the Melting Line to 700 K at Pressures up to 1000 MPa. J. Phys. Chem. Ref. Data 28, 779–850.

Vinš, V., Jäger, A., Hrubý, J., Span, R., 2017. Model for gas hydrates applied to CCS systems Part II. Fitting of the model parameters. Fluid Phase Equilib. 435, 104–117.

Vinš, V., Jäger, A., Span, R., Hrubý, J., 2016. Model for gas hydrates applied to CCS systems Part I. Parameter study of the van der Waals and Platteeuw model. Fluid Phase Equilib. 427, 268–281.

Wagner, W., Kretzschmar, H.-J., 2007. International Steam Tables - Properties of Water and Steam based on the Industrial Formulation IAPWS-IF97: Tables, Algorithms, Diagrams, and CD-ROM Electronic Steam Tables - All of the equations of IAPWS-IF97 including a complete set of supplementary backward equations for fast calculations of heat cycles, boilers, and steam turbines. Springer Berlin Heidelberg.

Wagner, W., Pruß, A., 2002. The IAPWS Formulation 1995 for the Thermodynamic Properties of Ordinary Water Substance for General and Scientific Use. J. Phys. Chem. Ref. Data 31, 387–535.

Wagner, W., Riethmann, T., Feistel, R., Harvey, A. H., 2011. New Equations for the Sublimation Pressure and Melting Pressure of H_2O Ice Ih. J. Phys. Chem. Ref. Data 40, 043103.

Wexler, A., Hyland, R. W., Stewart, R., 1983. Thermodynamic properties of dry air, moist air and water and SI psychrometric charts. ASHRAE.

Wilson, G. M., 1968. A modified Redlich-Kwong Equation of State: Application to General Physical Data Calculations. In: AIChE 65^{th} National Meeting. Cleveland, OH, May 4-7. No. 15C.

Yasuda, K., Oto, Y., Shen, R., Uchida, T., Ohmura, R., 2013. Phase equilibrium condition measurements in nitrogen and air clathrate hydrate forming systems at temperatures below freezing point of water. J. Chem. Thermodyn. 67, 143–147.

Zhang, Z., Pate, M. B., 1988. A Methodology for Implementing a Psychrometric Chart in a Computer Graphics System. DA-88-28-4. ASHRAE.